

EUROPEAN COOPERATION  
IN THE FIELD OF SCIENTIFIC  
AND TECHNICAL RESEARCH

---

COST 2100 TD(08) 511  
Trondheim, Norway  
2008/June/4-6

EURO-COST

---

SOURCE: AWE Communications GmbH,  
Germany

## **MIMO Channel Characteristics Computed with 3D Ray Tracing Model**

Oliver Stabler  
AWE Communications GmbH  
Otto-Lilienthal-Strae 36,  
71034 Boeblingen  
GERMANY  
Phone: + 49-7031 71497 19  
Fax: + 49-7031 71497 12  
Email: [Oliver.Staebler@AWE-Communications.com](mailto:Oliver.Staebler@AWE-Communications.com)

# MIMO Channel Characteristics Computed with 3D Ray Tracing Model

Oliver Stabler, Reiner Hoppe

AWE Communications, Otto-Lilienthal-Strae 36, 71034 Boblingen, Germany.

**Abstract** - Future wireless communication systems are expected to offer highly reliable broadband radio access in order to meet the increasing demands of emerging high speed data and multimedia services. In recent years information theoretic investigations have shown that multiple-input multiple-output (MIMO) systems can support extremely high data rates within rich scattering environments. To design high efficient MIMO wireless systems and predict system performance under various circumstances accurate MIMO wireless channel models for different scenarios are required. Recently, standardized double directional stochastic MIMO channel models have been proposed for different scenarios based on the statistical information evaluated from measured data. However, statistical channel models are based on measurement campaigns and therefore only valid for the measured scenarios.

In this paper the MIMO channel characteristics have been evaluated using deterministic channel modeling. A three dimensional ray tracing package has been utilized for the determination of the propagation paths and further crucial parameters of the radio channel, such as delay spread and angular spreads at both base and mobile stations.

**Keywords** - MIMO channel, deterministic channel modeling, ray tracing, channel matrix, channel capacity, Doppler spread.

## I. Introduction

In 3rd generation (3G) and beyond-3G (B3G) wireless communication systems higher data rate transmissions and better quality of services are demanded. In the last few years multiple-input multiple-output (MIMO) systems, which deploy spatially separated multiple antenna elements at both ends of the transmission link, have emerged as one of the most promising approaches for high data rate and more reliable wireless systems. Today several air interfaces are starting to become standardized in their respective standardization bodies (ETSI, 3GPP, IEEE). Besides a potential convergence at air interface level (OFDM or CDMA families), one might distinguish one common component across the different new and future air interface candidates: all of them take into account the MIMO technology. It was shown that the MIMO channel capacity grows linearly with antenna pairs as long as the environment provides sufficiently rich scattering effects. According to this, the capacity gains ultimately depend on the propagation channel in which the system is operating. For attaining or at least approaching those capacities, sophisticated signal processing algorithms and coding strategies have been developed and corresponding research is on going. In order to assess the benefits and possible problems of these algorithms, realistic models of the wireless propagation channel are required. Hence, the

establishment of good spatial channel models is essential both for the development of new algorithms for signal processing, modulation, coding, and for the unified testing of different system proposals in standardization.

## II. Deterministic Channel Modeling

Deterministic propagation models are generally based on ray-optical techniques where different rays emitted by the transmitting antenna are subject to reflection, scattering and diffraction at walls and edges of buildings and similar obstacles. The computations are performed with help of the universal theory of diffraction (UTD) and Fresnel coefficients for reflections or with empirical diffraction/reflection models. While empirical models for urban scenarios assume a dominant propagation from the transmitter to the receiver over the buildings' rooftops, deterministic models consider the physical 3D propagation paths. As a consequence, deterministic models cope with effects such as shadowing behind walls, wave guiding in street canyons, offer excellent accuracy and are able to provide additional parameters such as small-scale fading, delay and angular spreads.

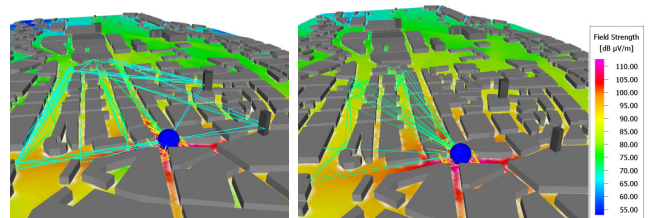


Figure 1: Multi path propagation below (left part) and above (right part) roof top level

The WinProp 3D ray tracing software [5] used for the deterministic modeling is based on the evaluation of 3D building data representing the considered environment (see Figure 1). The ray tracing propagation model is fully three dimensional and computes all rays with up to three interactions (incl. double diffraction, also in combinations with reflections). These settings lead to the best relation between computational effort and accuracy [1], [2].

## III. MIMO Radio Channel

In general, the radio propagation in urban environments is subject to multi path, i.e. the signal from the transmitter propagates along different paths to the (mobile) receiver. In many cases there is no direct line-of-sight (LOS) and the only

paths connecting transmitter and receiver are reflected, diffracted and scattered at a number of different obstacles (see Figure 1).

The radio propagation can be characterized by the impulse response of the radio channel between the position of the transmitter (Tx) and the position of the receiver (Rx). This impulse response consists of all individual multi path components (MPCs) and also represents their temporal and angular properties (see Figure 2).

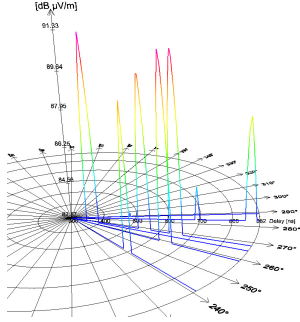


Figure 2: Spatial channel impulse response

There is a complex single-input single-output (SISO) channel impulse response of length  $L + 1$  between each transmit antenna  $m$  and each receive antenna  $n$  of a MIMO system.

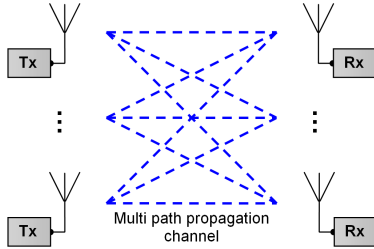


Figure 3: Model of the MIMO radio channel

$$h_{n,m}(t) = \sum_{\tau=0}^L h_{n,m,\tau}(t) \quad (1)$$

The linear time-variant MIMO channel is represented by the MIMO channel matrix of dimension  $N_R \times N_T$ .

$$H(t) = \begin{pmatrix} h_{11}(t) & \dots & h_{1,N_T}(t) \\ \dots & \dots & \dots \\ h_{N_R,1}(t) & \dots & h_{N_R,N_T}(t) \end{pmatrix} \quad (2)$$

$$\text{with } h_{n,m}(t) = \text{Re}\{h_{n,m}(t)\} + j \text{Im}\{h_{n,m}(t)\}. \quad (3)$$

### A. Determination of the MIMO Channel Matrix

The main disadvantage of deterministic wave propagation models is their excessive computation time. The most time-consuming part is the determination of all relevant paths from transmitter to receiver. Typically the spacing between the antenna elements is rather small (a few wave lengths at a maximum) and accordingly it can be assumed that the same multi paths exist for all antenna elements of the array. This means the power of each multi path contribution can be

considered as constant at each antenna element and also the angles of arrival (AoA) and departure (AoD). Only the phase of each multi path contribution is changing from one element to the other (assuming plane wave incidence), as illustrated in Figure 4. The phase shift  $\varphi$  between the center of the array and the antenna elements can be computed based on the angle of arrival (or departure) and the orientation of the array according to equation (4).

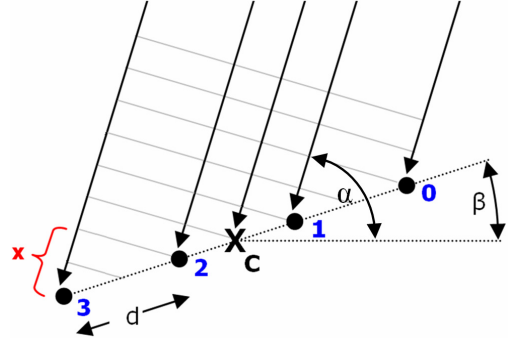


Figure 4: Uniform linear MIMO array with four antenna elements

$$\varphi = \frac{360^\circ}{\lambda} \cdot k \cdot \frac{d}{2} \cdot \cos(\alpha - \beta), \quad (4)$$

where  $\lambda$  is the wavelength,  $k \in [1,3,5,\dots]$ .

Equation (4) holds for arbitrary adjusted uniform linear MIMO antenna arrays with antenna elements located in one horizontal plane. Based on the uniform linear array it is also possible to determine the phase shifts between the elements of circular antenna arrays, by simply adjusting the angle of incidence in the equation above, according to the location of the antenna element on the circle.

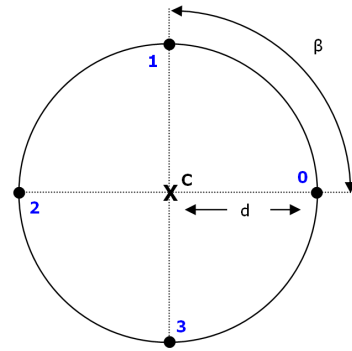


Figure 5: Circular MIMO array with four antenna elements

$$\varphi = \frac{360^\circ}{\lambda} \cdot d \cdot \cos(\alpha - i \cdot \beta), \quad (5)$$

where  $\lambda$  is the wavelength,  $i \in [0,1,2,3,\dots]$ .

Such a modular approach will avoid re-computing the ray tracing between all the antenna elements of transmitter and receiver station. However, in case of large spacing (e.g.  $> 10 \lambda$  at Tx) or specific configurations (e.g. incl. shielding between the individual elements) this methodology might introduce inaccuracies and shall therefore be replaced by the rigorous application of the ray tracing algorithm.

## B. MIMO Channel Capacity

As multiple-input multiple-output systems have emerged as one of the most promising approaches for high data rates, the channel capacity is a further significant parameter for the characterization of a MIMO system.

The standard formula for the Shannon capacity expressed in bits per second and hertz can be written as

$$C = \log_2 \left( 1 + \rho \cdot |H|^2 \right), \quad (6)$$

with  $\rho = P/N$  the average SNR at each receiver branch.

From this general expression the convenient general capacity expression for non-frequency selective MIMO channels can be derived as [3]:

$$C = \log_2 \left( \det \left[ I_{N_R} + \frac{P}{N_T \cdot \sigma_n^2} \cdot H_F \cdot H_F^H \right] \right), \quad (7)$$

with the unity matrix  $I$ , the overall transmit power  $P$  and the noise power  $\sigma_n^2$ .

The channel matrices  $H_F$  in equation (7) are determined by  $N_F$ -point Fast Fourier Transformation of the normalized channel power transfer characteristics, mentioned in chapter III.

The next generation of wireless communication systems, such as WiMAX and 3G LTE will use channel bandwidths up to 20 MHz for transmission. Those broadband channels have to be considered as frequency selective channels, i.e. equation (7) is no longer valid for capacity estimation of such channels. For frequency selective MIMO channels, the channel capacity can be obtained by integrating over the non-frequency selective sub-channels. For the discrete case, capacity estimation can be determined by averaging the non-frequency selective sub-channels. The resulting formula is shown in equation (8).

$$C = \frac{1}{N_F} \sum_{l=0}^{N_F-1} \log_2 \left( \det \left[ I_{N_R} + \frac{P}{N_T \cdot \sigma_n^2} \cdot H_F(l) \cdot H_F(l)^H \right] \right), \quad (8)$$

with the unity matrix  $I$ , the overall transmit power  $P$  and the noise power  $\sigma_n^2$ .

For the comparison of different MIMO channels, the power of the single channels has to be normalized.

$$\sum_{\tau=0}^L E \left\{ |h_{n,m,\tau}(t)|^2 \right\} = 1 \xrightarrow{FFT} \sum_{l=0}^{N_F-1} E \left\{ |H_{F,n,m}(l)|^2 \right\} = N_F \quad (9)$$

In order to normalize a MIMO channel according to equation (9), every SISO channel has to be multiplied with a different normalization factor. This means, the path loss of each SISO channel would be rated differently. Hence the condition in (9) is extended to a normalization rule for a comparability based on the same signal-to-noise-ratio (SNR) [4].

$$\sum_{n=1}^{N_R} \sum_{m=1}^{N_T} \sum_{l=0}^{N_F-1} |H_{n,m}(l)|^2 = N_R \cdot N_T \cdot N_F \quad (10)$$

Equation (10) introduces one normalization factor for all SISO channels, which obviously differs from system to system. By adding a further factor to equation (10), a normalization factor for  $N_C$  different MIMO channels can be obtained [4].

$$\sum_{c=1}^{N_C} \sum_{n=1}^{N_R} \sum_{m=1}^{N_T} \sum_{l=0}^{N_F-1} |H_{c,n,m}(l)|^2 = N_C \cdot N_R \cdot N_T \cdot N_F \quad (11)$$

However, the estimated channel capacity is calculated for every single MIMO channel, which does not necessarily fulfill condition (10) when the system has been normalized with equation (11). This causes additional noise for each MIMO channel, resulting in different signal-to-noise-ratios.

It is not possible to fulfill both normalization conditions at the same time, therefore the system can either be normalized for a comparison based on the same SNR (10) or for a comparison based on the same path loss (11).

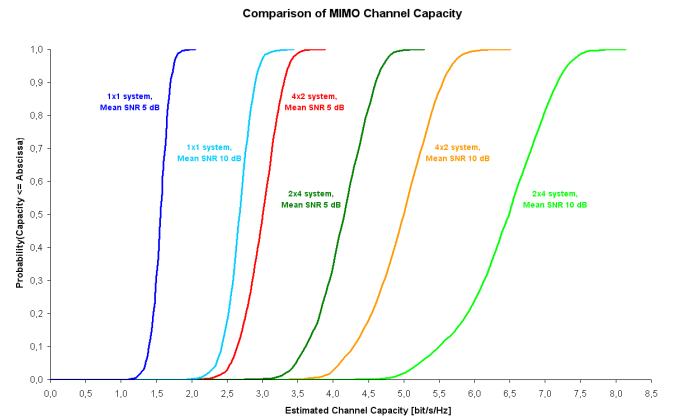


Figure 6: Capacity comparison of different MIMO configurations (in urban scenario)

Figure 6 compares the cumulated probability density functions of different MIMO systems. The estimated capacities are determined using the normalization condition (10) for a comparison based on the same SNR. With the increase of the mean SNR from 5 dB to 10 dB the capacity rises with a factor of 1.6. It can be shown, that receive diversity offers significant capacity improvement in contrast to transmit diversity. Figure 6 indicates an estimated channel capacity of 5.0 bit/s/Hz (median value) for a 4x2 MIMO system and 6.5 bit/s/Hz (median value) for a 2x4 MIMO system respectively, under consideration of the same mean SNR.

## C. Influence of mutual antenna coupling

Mutual coupling between the antenna elements of a MIMO array is an important factor to be taken into account for an accurate modelling of the transmission channel. Due to space limitations, especially in portable devices, multiple antennas

often have to be placed close together. Thus, mutual coupling between antennas is generated and can have a significant impact on MIMO transmission characteristics.

To model the influence of the mutual antenna coupling, two correlation matrices  $R$  are introduced, which represent the antenna coupling effects at the transmitter and the receiver antenna array respectively.

$$R_i = \begin{bmatrix} 1 & \rho_{i,12}^* & \dots & \rho_{i,1N_T}^* \\ \rho_{i,21} & 1 & \dots & \rho_{i,2N_T}^* \\ \dots & \dots & \dots & \dots \\ \rho_{i,N_R1} & \rho_{i,N_R2} & \dots & 1 \end{bmatrix}, \quad (12)$$

where  $i$  stands for Tx or Rx antenna array.

The complex correlation coefficients are based on the spacing between the two considered antenna elements of an array and the occurring power angular spectrum (PAS).

$$\begin{aligned} \text{Re}\{\rho_{i,j,k}\} &= \int_{-\pi}^{\pi} \cos\left(\frac{2\pi \cdot d}{\lambda} \cdot \sin(\varphi)\right) \cdot \text{PAS}(\varphi) d\varphi, \\ \text{Im}\{\rho_{i,j,k}\} &= \int_{-\pi}^{\pi} \sin\left(\frac{2\pi \cdot d}{\lambda} \cdot \sin(\varphi)\right) \cdot \text{PAS}(\varphi) d\varphi, \end{aligned} \quad (13)$$

with spacing  $d$  between antenna element  $j$  and  $k$ .

To correlate the entries of the MIMO channel matrix  $H$  (see section A), the following method can be used.

$$H_c = R_{R_x}^{1/2} \cdot H \cdot R_{T_x}^{1/2} \quad (14)$$

## IV. MIMO Channel Evaluations

### A. Influence of mutual antenna coupling

This section shows the influence of mutual antenna coupling on the MIMO channel matrices. A 4x2 MIMO system, operating at a frequency of 2 GHz, has been evaluated in an urban environment. The uniform linear transmitter array consists of four elements with spacing of 10 Lambda and is located 14 meters above the ground (below rooftop of surrounding buildings). The receiver is also equipped with a uniform linear array, but has only two antenna elements located 1.5 meters above street level (red arrow in Figure 7).

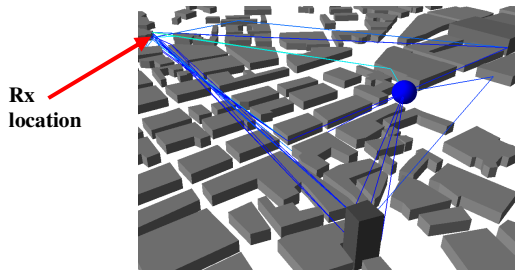


Figure 7: Simulation scenario

Figure 8 depicts the absolute values of the resulting antenna correlation coefficients between the first and the second antenna element of Tx and Rx antenna array depending on the distance between the elements. It can be seen, that correlation decreases rapidly with increasing antenna spacing. For BS above rooftop larger differences in correlation coefficients are expected.

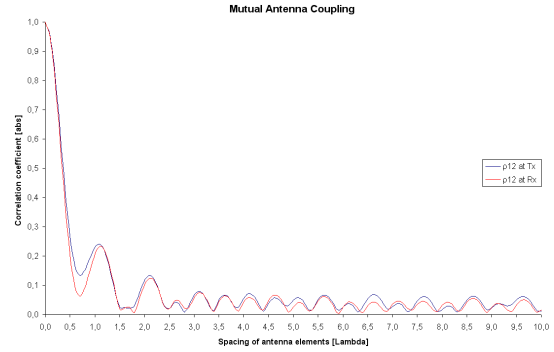


Figure 8: Correlation coefficients at Tx and Rx array

The following polar charts show the difference between the correlated and the uncorrelated MIMO channel matrix for the given receiver location. The blue points denote the resulting matrix entries of the channel matrix including mutual antenna coupling, the red color stands for the corresponding uncorrelated entries.

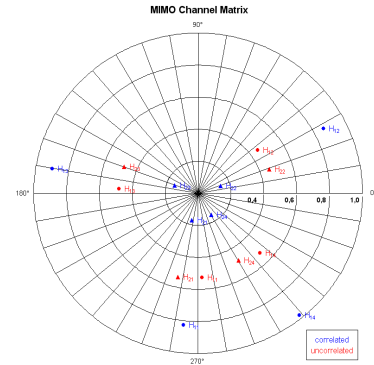


Figure 9: MIMO channel matrix with and without influence of mutual antenna coupling for an Rx antenna spacing of 0.1 Lambda

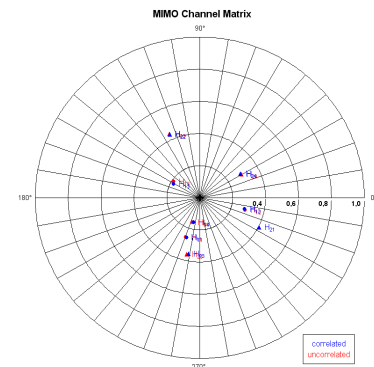


Figure 10: MIMO channel matrix with and without influence of mutual antenna coupling for an Rx antenna spacing of 10 Lambda

For an antenna spacing of 10 Lambda (1.5 meter), the absolute values of the correlation coefficients at Tx and Rx array are below 0.02, which results in a low difference

between correlated and uncorrelated MIMO channel matrix (see Figure 10). However, mutual antenna coupling has a large impact for small spacing (see Figure 8). A spacing of 0.1 Lambda for example results in two completely different channel matrices (see Figure 9).

## B. Receiver Moving on a Trajectory

The following section shows a 4x2 MIMO system with a receiver, for example a car, moving along a trajectory within an urban environment. The system is operating at a frequency of 2.5 GHz. The transmitter uses a uniform linear MIMO array with four antenna elements located on a building, 25 meters above the ground (see Figure 11). The receiver starts his journey at a velocity of 0 m/s (1, center of Figure 11) and accelerates along the trajectory up to 19.45 m/s.

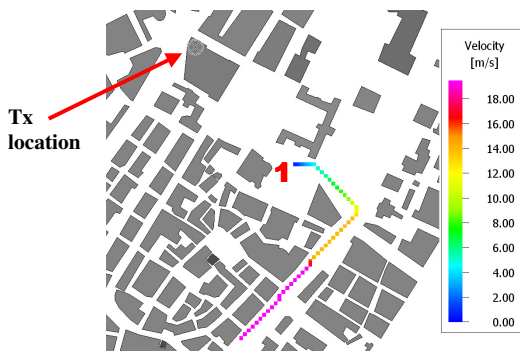


Figure 11: Simulation scenario with trajectory of the receiver

Figure 12 illustrates the estimated channel capacity along the evaluated trajectory starting at point 1 (see Figure 11). For the determination of the channel capacities a mean signal-to-noise-ratio of 15 dB was assumed. The MIMO systems have been normalized for a comparison based on the same SNR (see eq. (10)).

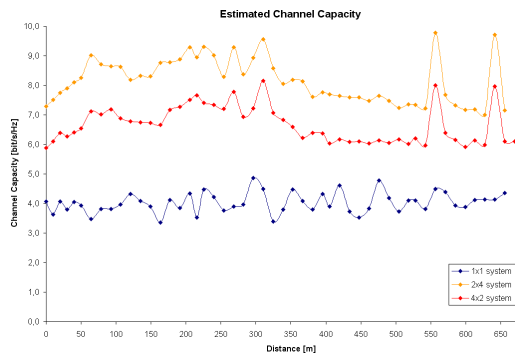


Figure 12: Estimated channel capacity along the trajectory

Three different MIMO system configurations have been plotted for comparison. The blue line on the bottom represents the channel capacity reachable for a 1x1 system. This system can reach an average estimated channel capacity of 4.0 bit/s/Hz. Using a MIMO system with four transmit and two receive antenna elements (red line in Figure 12) instead, the average estimated channel capacity can be increased to 6.7 bit/s/Hz. A further enhancement can be achieved by increasing the number of receiver elements.

TABLE I  
COMPARISON OF ESTIMATED CHANNEL CAPACITY ALONG THE TRAJECTORY FOR A MEAN SNR OF 15 dB

MIMO System	Min Capacity	Max Capacity	Average Capacity
1 x 1	3.4 bit/s/Hz	4.9 bit/s/Hz	4.0 bit/s/Hz
2 x 4	7.0 bit/s/Hz	9.8 bit/s/Hz	8.2 bit/s/Hz
4 x 2	5.9 bit/s/Hz	8.2 bit/s/Hz	6.7 bit/s/Hz

The following figure shows the occurring Doppler spreads (blue line in Figure 13) along the trajectory. The orange line denotes the velocity of the receiver.

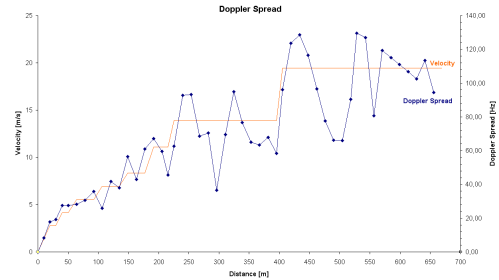


Figure 13: Doppler spread along the trajectory

As the Doppler spread is inversely proportional to the coherence time of the channel, the values increase with increasing velocity of the receiver station, i.e. with incremental fluctuations of the channel properties.

## V. Acknowledgements

This work has been supported by the German Ministry for Education and Research (BMBF) within the EUREKA MEDEA+ project MIMOWA, which is kindly acknowledged.

## VI. References

- [1] T. Rautiainen, G. Wölfle, and R. Hoppe: “Verifying Path Loss and Delay Spread Predictions of a 3D Ray Tracing Propagation Model in Urban Environments”, 56th IEEE Vehicular Technology Conference (VTC) 2002 - Fall, Vancouver, Canada, September 2002.
- [2] R. Hoppe, J. Ramulu, H. Buddendick, O. Stäbler, and G. Wölfle: “Comparison of MIMO Channel Characteristics Computed by 3D Ray Tracing and Statistical Models”, 2nd European Conference on Antennas and Propagation (EuCAP 2007), Edinburgh, UK, November 2007.
- [3] G. J. Foschini and M. J. Gans, “On Limits of Wireless Communication in a Fading Environment when Using Multiple Antennas,” *Wireless Personal communications*, vol. 6, pp. 311–335, March 1998.
- [4] F. Hageböling, O. Weikert, U. Zölzer: “Deterministic Prediction of the Channel Capacity of Frequency Selective MIMO Systems”, *Proc. 11th International OFDM-Workshop 2006 (InOWo'06)*, Hamburg, Germany, August 2006.
- [5] AWE Communications: WinProp Software Package. Free evaluation version of a 3D ray tracing tool for urban and indoor environments. Available: <http://www.awe-communications.com>